

What’s the Magic Word? A CONTROL THEORY OF LLM PROMPTING

Aman Bhargava¹, Cameron Witkowski², Manav Shah², Matt Thomson¹ *

¹California Institute of Technology, ²University of Toronto

{abhargav, mthomson}@caltech.edu

{cameron.witkowski, manav.shah}@mail.utoronto.ca

ABSTRACT

Prompt engineering is effective and important in the deployment of LLMs but is poorly understood mathematically. Here, we formalize prompt engineering as an optimal control problem on LLMs – where the prompt is considered a **control variable** for modulating the output distribution of the LLM. Within this framework, we ask a simple question: *given a sequence of tokens, does there always exist a prompt we can prepend that will steer the LLM toward accurately predicting the final token?* We call such an optimal prompt the *magic word* since prepending the prompt causes the LLM to output the correct answer. If *magic words* exist, can we find them? If so, what are their properties? We offer analytic analysis on the controllability of a self-attention head where we prove a bound on controllability as a function of the singular values of its weight matrices. We take inspiration from control theory to propose a metric called $k - \epsilon$ **controllability** to characterize LLM steerability. We compute the $k - \epsilon$ controllability of a panel of large language models, including Falcon-7b, Llama-7b, and Falcon-40b on 5000 WikiText causal language modeling tasks. Remarkably, we find that *magic words* of 10 tokens or less exist for over 97% of WikiText instances surveyed for each model.

1 INTRODUCTION

LLMs pre-trained on unsupervised next token prediction objectives exhibit unprecedented dynamic reprogrammability achieved through “prompting”, often referred to as zero-shot learning (Brown et al., 2020; Wei et al., 2022; Hagendorff, 2023; Noever & McKee, 2023; OpenAI, 2023; 2022). These capabilities appear to emerge as the model’s size, training data, and training time are scaled. The dynamic reprogrammability of LLMs is akin to the adaptable computational capacities observed in biological systems. This feature finds applications across domains such as machine translation (Wang et al., 2023a), code generation (Rozière et al., 2023), and chatbots Bai et al. (2022). A rigorous understanding of the prompt’s influence over LLM generation would be of great utility for understanding LLMs and building more robust and capable systems leveraging LLMs.

Strategies for controlling pre-trained LLM generation today fall into three broad categories (Zhang et al., 2022):

1. **Input Optimization:** Adjusting the input tokens (e.g., rewording the prompt) to improve subsequent text generation.
2. **Model Optimization:** Adjusting the weights of the network (e.g., re-training, fine-tuning, RLHF) to improve model behavior during inference.
3. **Post-processing:** Adjusting or re-ranking generated text (e.g., surrogate ranking algorithm).

Of all these approaches, input optimization (i.e., prompting) is the least invasive and lowest-cost method – and the least understood. Prompt optimization is also deeply connected to the zero-shot

*Code will be made available at https://github.com/amanb2000/Magic_Words.

capabilities of LLMs, the mysterious, emergent problem-solving, knowledge, and reasoning abilities exhibited by large scale models. With such a view, we seek to characterize the controllability of LLMs via prompting.

We ask a simple question: *does there exist a “magic word” for any given next-token prediction task, such that when the magic word is prepended, the model will output the correct answer?* If there is, how long must the magic word be to steer the model to correct answer? How hard is it to find the magic words?

To approach these questions, we invoke the conceptual and mathematical machinery of control theory and define a notion of controllability for LLMs called $k - \epsilon$ **controllability** in section 3. In section 4 we offer a mathematical analysis on the controllability of a single attention head where we prove a bound on controllability as a function of the singular values of the weight matrices. In section 5 we describe two methods to find *magic words*, which we use to ascertain the controllability of Falcon-7b, Llama-7b, and Falcon-40b. Our results are presented in section 6. Remarkably, we find that there generally exists a *magic word* of length 10 or less for over 97% of Wikipedia causal language modelling instances surveyed.

2 RELATED WORK

Much of the work on prompt optimization is concerned with finding prompts that induce higher LLM performance on “fill-in-the-blank” or “cloze” tasks (Taylor, 1953). One can frame a range of tasks including knowledge retrieval (Petroni et al., 2019), reasoning (Weston et al., 2016), and sentiment analysis (Wang et al., 2023b) as fill-in-the-blank tasks:

- **Knowledge Retrieval:** “*The Titanic sank in the year [MASK].*” (Answer: “1912”)
- **Reasoning:** “*A is taller than B. B is taller than C. Is A taller than C? Answer: [MASK]*” (Answer: “Yes”)
- **Sentiment Analysis:** “*I am sad today. The sentiment of the previous sentence was [MASK]*” (Answer: “Negative”)

Notably, there is some freedom in the bolded “prompt text” that surrounds the question to convert it into a “fill-in-the-blank” task. As it turns out, the prompt tokens have a large effect on LLM performance (Brown et al., 2020; Zhang et al., 2022; Jiang et al., 2020).

Modern prompt optimization algorithms generally consist of two iterated steps: a sampling step where new prompts are generated and a testing step where the utility of the new prompts is evaluated, and the best are selected for the next iteration. Algorithms primarily differ in the sampling procedure, where various heuristics may be used to pick high-value swaps (Wen et al., 2023; Zhou et al., 2023; Reynolds & McDonell, 2021). Overall, AutoPrompt and its derivative algorithms have been the most numerically successful prompt optimization methods, with the greedy coordinate gradient (GCG) algorithm having state-of-the-art performance (Zou et al., 2023).

The AutoPrompt Family: AutoPrompt (Shin et al., 2020) pioneered the current wave of prompt optimization. Shin *et al* propose a prompt optimization technique and demonstrate its effectiveness for engineering prompts to improve LLM performance on knowledge and sentiment analysis tasks. At its core, the AutoPrompt algorithm leverages gradient information at the token embedding layer to inform iterative token exchanges within the prompt. This method was extended in Zou et al. (2023) as the greedy coordinate gradient (GCG) algorithm. Taking inspiration from adversarial examples (Goodfellow et al., 2015), Zou *et al* applied this AutoPrompt variant to generate “jailbreak” prompts that cause aligned LLMs to generate objectionable content.

Other Prompt Optimization Methods: Other investigations on LLMs as prompt optimizers (Zhou et al., 2023) and further analysis of manual prompt optimization (Reynolds & McDonell, 2021) are informative but do not exceed the AutoPrompt family’s performance. Some other methods include GBDA (Guo et al., 2021), an approach based on the Gumbel-Softmax reparametrization, the PEZ algorithm (Wen et al., 2023), which directly optimizes embeddings via gradient information, and FluentPrompt (Shi et al., 2022), which differs from AutoPrompt by incorporating Langevin dynamics. Despite the variety of alternatives, GCG retains state-of-the-art performance.

3 CONTROL THEORY FOR LLMs

Control theory originates from the study of automatic control systems in engineering. It seeks to understand how a “plant” system can be influenced toward a desired state using a “control signal” – often in the presence of disturbances and uncertainty.

Control theory is central to a variety of engineering problems, from autopilot to telecommunications to manufacturing. Surprisingly, control theory has also been highly applicable to a diverse range of scientific disciplines. Analyzing systems through the lens of controllability has proven fruitful for generating insight into biological systems such as cell signaling pathways and neural networks (Yi et al., 2000), the economics of central banking (Anița et al., 2011), and controlling the spread of infectious diseases (Roy et al., 2009). One of the central benefits of studying systems via controllability is that a range of questions and problems naturally emerge from the framing: *when is control possible? What is the cost of control? How computationally intensive is control?* These questions are both practically useful and often lead to fundamental insights about the nature of the system in question.

To build a control theory of LLMs, we begin with an abstract definition of systems and control, then outline specific canonical control problems that arise naturally for LLM systems.

3.1 ABSTRACT SYSTEMS AND CONTROL

Diverse definitions of “system” or “machine” exist in the literature, all representing the same core concept but varying in mathematical details. We offer the following high-level definition based on Sontag (2013):

Definition 1: System A “system” or “machine” $\Sigma = (\mathcal{T}, \mathcal{X}, \mathcal{U}, \phi)$ consists of:

- \mathcal{T} : The **time set** along which system state evolves.
- \mathcal{X} : The **state space**.
- \mathcal{U} : The **input space**.
- $\phi : \mathcal{X} \times \mathcal{U} \times \mathcal{T}^2 \rightarrow \mathcal{X}$: The **transition map**.

A system may also be equipped with an output space and readout map (\mathcal{Y}, h) :

- \mathcal{Y} : The **output space**.
- $h : \mathcal{X} \times \mathcal{U} \times \mathcal{T} \rightarrow \mathcal{Y}$: The **readout map**.

In other words, at time $t \in \mathcal{T}$, the system’s state takes on values $x \in \mathcal{X}$, and the control input takes values $u \in \mathcal{U}$. The system evolves over time with the transition map $\phi(x, u, t, t')$ that returns the new state value $x' \in \mathcal{X}$ at time $t' > t$. A system can also have a readout map $h(x, u, t)$ that produces the output value $y \in \mathcal{Y}$ given the current time, state, and input value.

A wide variety of systems are expressible within this framework. E.g., for $\mathcal{T} = \mathbb{Z}^+$, we obtain discrete dynamical systems. For $\mathcal{T} = \mathbb{R}^+$ and in the limit as $t' \rightarrow t$, continuous dynamical systems emerge.

Diverse definitions of controllability also exist in the literature, often specific to a certain class of system (e.g., continuous or discrete systems). At their core, all definitions revolve around the existence of control inputs $u \in \mathcal{U}$ that steer the system from a starting state to a desired state.

Definition 2: State controllability A system $\Sigma = (\mathcal{T}, \mathcal{X}, \mathcal{U}, \phi)$ is **state controllable** if, for any initial state $x_0 \in \mathcal{X}$ and desired final state $x_f \in \mathcal{X}$, there exists a control input $u^* \in \mathcal{U}$ such that the state is steered to x_f in finite time.

A similar controllability definition called “output controllability” is frequently used for systems equipped with a readout map $h : \mathcal{X} \times \mathcal{U} \times \mathcal{T} \rightarrow \mathcal{Y}$.

Definition 3: Output controllability A system $\Sigma = (\mathcal{T}, \mathcal{X}, \mathcal{U}, \phi, \mathcal{Y}, h)$ is **output controllable** if, for any initial output $y_0 \in \mathcal{Y}$ and desired final output $y_f \in \mathcal{Y}$, there exists a control input $u^* \in \mathcal{U}$ such that the output is steered to y_f in finite time.

A range of fruitful questions stem from these definitions: if there is a cost associated with control inputs $u \in \mathcal{U}$ (e.g., power constraints, length constraints), what is the minimum cost of control? What are the bounds on control time? If the system is not completely controllable, under what conditions is it controllable? Under which readout maps is a system output controllable?

With these questions in mind, we apply this abstract control theoretic framework to LLM systems.

3.2 LLM SYSTEMS AND CONTROL

We use P_{LM} to denote a causal language model. P_{LM} accepts an ordered list of tokens from a vocabulary set \mathcal{V} (e.g., $x \in \mathcal{V}^n$) and computes the probability distribution over the next token $P_{LM}(x_{n+1}|x) \in [0, 1]^{|\mathcal{V}|}$. We use \mathcal{V}^* to denote the set of all possible strings of any length composed of tokens from \mathcal{V} . The addition operator indicates the concatenation of token sequences.

The general system Definition 1 is applicable to a range of LLM configurations – including chain-of-thought systems (Wei et al., 2023), tool-wielding LLMs (Cai et al., 2023), interactive chatbots (Bai et al., 2022), and even LLMs with stochastic sampling. We begin with a deterministic system with a single output. For simplicity, the time set \mathcal{T} and the transition map ϕ are omitted from this definition.

Definition 4: Single-output zero-temperature LLM system A single-output zero-temperature LLM system $\Sigma = (\mathcal{X}, \mathcal{U}, \mathcal{Y}, h)$ based on causal language model P_{LM} with vocabulary \mathcal{V} consists of

- $\mathcal{X} = \mathcal{V}^*$: The **state space** is the set of all possible token sequences from vocabulary \mathcal{V} .
- $\mathcal{U} = \mathcal{V}^*$: The **input space** is the set of all possible token sequences from \mathcal{V} .
- $\mathcal{Y} = \mathcal{V}$: The **output** takes on single-token values from the vocabulary.
- $h(x, u) = \arg \max P_{LM}(y|u + x)$: The **readout map** takes the argmax of the distribution over the next token y given the control token sequence u and the state token sequence x .

Definition 5: Output controllability for single-output zero-temperature LLM system Following from Definition 3, an LLM system is output controllable if, for any imposed state $x \in \mathcal{V}^*$ and desired $y^* \in \mathcal{V}$, there exists some $u^* \in \mathcal{V}^*$ such that $h(x, u^*) = y^*$.

Due to the costly nature of long prompts, we are especially interested in the existence of prompts u^* with minimal length $|u^*|$. Since exhaustive testing of controllability on all sequences in \mathcal{V}^* is intractable, we propose the following continuous measure of controllability for practically assessing the steerability of LLMs.

Definition 6: $k - \epsilon$ controllability – A single-output zero-temperature LLM system is $k - \epsilon$ controllable at prompt length $|u^*| \leq k$ w.r.t. text distribution $P_{\mathcal{D}}$ if the probability that some text sequence $(x + y) \sim P_{\mathcal{D}}$ has no optimal control u^* of length $|u^*| \leq k$ such that $h(x, u^*) = y^*$ is ϵ .

In other words, $k - \epsilon$ controllability measures the probability ϵ that there is **no optimal prompt** u^* of length k or less that will force the final token prediction $\arg \max_{y'} P(y'|u + x)$ to be the correct value. $\epsilon = 0$ corresponds to complete controllability while $\epsilon = 1$ corresponds to complete uncontrollability. We may compute upper bound estimates for $k - \epsilon$ controllability by finding minimum length optimized prompts for eliciting the correct final token for each element of a dataset of sequences drawn from some $P_{\mathcal{D}}$ (see section 5 for our specific methods section 6 for our results).

We call an optimal control prompt u^* the *magic word*. Prepending the *magic word* to the model input causes it to output the correct answer.

One can define a range of LLM systems and controllability definitions based on the model requirements and the problem at hand. We discuss these alternatives at length in section 7. The most general form of prompt-based controllability is **complete state control**: let us consider an LLM

system where we seek to control the internal representation $\mathcal{I}(x|u)$ (intermediate transformer activations including logits associated with tokens x conditioned on u) computed in the operation of the transformer $P_{LM}(\cdot|\cdot)$:

Definition 7: State controllability – *An LLM system is completely state controllable if, for any imposed sequence $x \in \mathcal{X}$ and a desired internal representation \mathcal{I}^* , there exists some u^* such that $\mathcal{I}(x|u^*) = \mathcal{I}^*$.*

This is a far deeper level of control and is likely intractable with current LLM technology. However, we found it to be a productive framing for proving bounds on the controllability of a self-attention head as a function of the singular values of its parameter matrices in section 4. In section 6, we compute $k - \epsilon$ controllability for a panel of models, showing that optimal prompts u^* exist with length $k \leq 10$ over 97% of the Wikitext sequences ($\epsilon < 0.03$).

4 MATHEMATICAL ANALYSIS ON THE CONTROLLABILITY OF SELF-ATTENTION

The self-attention head is a defining component of modern transformer-based language model architectures. It is the component where information arising at different token positions is mixed together. To understand the complete state controllability (Definition 7) of LLMs, we start by analyzing the conditions under which a self-attention head is completely controllable.

We denote the operation of a self-attention head with input $\mathbf{X} \in \mathbb{R}^{(N+M) \times d_{in}}$ as follows:

$$\text{Self-Attention}(\mathbf{X}) = \text{softmax}\left(\frac{\mathbf{X}\mathbf{W}_q(\mathbf{X}\mathbf{W}_k)^\top}{\sqrt{d_k}}\right)\mathbf{X}\mathbf{W}_v \quad (1)$$

$$\mathbf{X}' = \text{softmax}\left(\frac{\mathbf{Q}\mathbf{K}^\top}{\sqrt{d_k}}\right)\mathbf{V} \quad (2)$$

where $\mathbf{W}_q, \mathbf{W}_k$ are linear maps from dimension d_{in} to d_k and \mathbf{W}_v is a linear map from d_{in} to d_{out} . $\mathbf{Q} = \mathbf{X}\mathbf{W}_q \in \mathbb{R}^{(N+M) \times d_k}$ are queries, $\mathbf{K} = \mathbf{X}\mathbf{W}_k \in \mathbb{R}^{(N+M) \times d_k}$ are keys, and $\mathbf{V} = \mathbf{X}\mathbf{W}_v \in \mathbb{R}^{(N+M) \times d_{out}}$ are values. $\mathbf{X}' \in \mathbb{R}^{(N+M) \times d_{out}}$ denotes the transformed version of \mathbf{X} (Vaswani et al., 2017).

We partition the input tokens into a modifiable input subset $\mathbf{u}_1 \dots \mathbf{u}_N$ (denoted \mathbf{u}) and a fixed subset $\mathbf{x}_1 \dots \mathbf{x}_M$ (denoted \mathbf{x}).

$$\mathbf{X} = \begin{bmatrix} \mathbf{u} \\ \mathbf{x} \end{bmatrix} \quad \mathbf{X}' = \begin{bmatrix} \mathbf{u}' \\ \mathbf{x}' \end{bmatrix} \quad (3)$$

We consider \mathbf{x}' the output of the system. Our goal is to understand the conditions under which the system is **state controllable** (Definition 7). Specifically, we ask the following question:

For any imposed \mathbf{x} and any desired \mathbf{x}^ , does there exist an input sequence \mathbf{u}^* that will force the resulting $\mathbf{x}' = \mathbf{x}^*$?*

Assuming that each row vector $\mathbf{u}_i, \mathbf{x}_i$ is confined to $\|\mathbf{u}_i\| \leq 1$ and $\|\mathbf{x}_i\| \leq 1$, we obtain the following bound on controllability. If this condition is met for any $i \in 1 \dots M$, then the attention head is **not state controllable**:

$$\sigma_{\max}(W_v) < \left\| \mathbf{x}_i^* + \left(\frac{D_i^{(2)}}{N \exp\left(\frac{\sigma_{\max}(W_q)\sigma_{\max}(W_k)}{\sqrt{d_k}}\right)} \right) (\mathbf{x}_i^* - \hat{\mathbf{x}}_i^{(2)}) \right\| \quad (4)$$

Where

- $\sigma_{\max}(\cdot)$ is the largest singular value of a matrix
- \mathbf{x}_i^* is the i th row vector of the desired \mathbf{x}^* .

-
- $\hat{\mathbf{x}}^{(2)} = \text{Self-Attention}(\mathbf{x})$, the output of Self-Attention when only the imposed, uncontrollable input vectors \mathbf{x} are used as input. Each $\hat{\mathbf{x}}_i^{(2)}$ are row vectors of this output.
 - $D_i^{(2)}$ is a component of the row-wise softmax denominator corresponding to the imposed input \mathbf{x} given by

$$\sum_{\ell=1}^M \exp \left(\frac{\mathbf{x}_i \mathbf{W}_q \mathbf{W}_k^\top \mathbf{x}_\ell^\top}{\sqrt{d_k}} \right) \quad (5)$$

This result is proven in Appendix A. Thus we have expressed a controllability bound for the self-attention head solely in terms of the desired output values \mathbf{x}^* , the imposed inputs \mathbf{x} , the weight matrices of the attention head $\mathbf{W}_v, \mathbf{W}_k, \mathbf{W}_q$, and the number of controllable input vectors N .

This condition is liable to arise when $M \gg N$. Intuitively, this condition is met when the attention mechanism allocates a substantial amount of attention to the values arising from the uncontrolled $\mathbf{x}_1 \dots \mathbf{x}_M$ inputs (i.e., large $D_i^{(2)}$) with very few controllable inputs $\mathbf{u}_1 \dots \mathbf{u}_N$ to the point that even maximal attention allocation to the $\mathbf{u}_1 \dots \mathbf{u}_N$ values could not steer the system to the goal state. Excitingly, this result aligns with our findings in section 6 that ϵ (representing the proportion of uncontrollable instances) decreases with k and increases with the number of imposed tokens.

5 COMPUTATIONAL METHODS

To ascertain the $k - \epsilon$ controllability of a language model, we require a technique for computing k -long *magic words* $u^* \in \mathcal{V}^k$ for a given set of base tokens $x \in \mathcal{V}^*$ and desired answer token $y \in \mathcal{V}$. We also require a dataset of base token strings $(x + y) \sim P_{\mathcal{D}}$ to estimate the value of ϵ .

Inferring *magic words* by brute-force enumeration of all possible sequences in \mathcal{V}^k is intractable for $k > 1$. We therefore require heuristic search methods to find good *magic words*. We use two techniques for inferring *magic words*: greedy back-generation and greedy coordinate gradient (GCG, Zou et al. (2023)). To our knowledge, our greedy back-generation algorithm is novel. We sample base token strings $x + y$ from the Wikitext dataset (Merity et al., 2016) with lengths ranging from 8-32 tokens. Finally, we measure the $k - \epsilon$ controllability for Falcon-7b, Falcon-40b (Almazrouei et al., 2023), and Llama-7b Touvron et al. (2023).

Greedy Back-Generation: While testing all prompts in \mathcal{V}^k is intractable for $k > 1$, it takes only $|\mathcal{V}|$ forward passes of the network to compute the loss on y induced by all possible *single token* prompts $u \in \mathcal{V}$. Our Greedy Back Generation algorithm leverages this fact to generate prompts $u \in \mathcal{V}^k$ one token at a time, working backward sampling the i th greedy-optimal single token extension $u' = \arg \max_{u'} P_{LM}(y|u' + u + x)$ of the current prompt $u \in \mathcal{V}^{i-1}$. See Algorithm 1 in Appendix B for the exact pseudocode.

This method is optimal for $k = 1$ *magic word* token u^* and generally outperforms GCG for short prompts of length $k \leq 3$. Computing 1 additional prompt token takes roughly 1-4 minute when using an NVIDIA A100-80GB GPU with a 7 billion parameter model and 5-20 minutes on 2 NVIDIA A100-80GB GPUs with a 40 billion parameter model.

Greedy Coordinate Gradient (GCG): The Greedy Coordinate Gradient algorithm, presented by (Zou et al., 2023) building off the work of (Shin et al., 2020), is the state-of-the-art method for optimizing prompts. Starting with a random prompt of length k , the algorithm generates a batch of alternative prompts. Each member of the batch swaps a random token in the current prompt with a promising alternate token. The value metric for a swap is given by a first order approximation of the change in loss $\mathcal{L} = \text{CELoss}(y, P_{LM}(y|u + x))$ with the embedding of each token in u . Full pseudocode can be found in Algorithm 2 in Appendix B.

This method outperforms all other methods we tested for prompts of length $k > 3$. We use a batch size $B = 768$, sampled from the top $k_{sub} = 128$ token replacements at each index, and iterate for $T = 34$ iterations. For each instance, this optimization took roughly 2 minutes for the 7 billion parameter models on a single A100-80GB GPU and 4-8 minutes for the 40 billion parameter model on 4 A100-80GB GPU.

Wikitext Causal Language Modelling: To determine the controllability of a model, we select 5,000 strings for the 7 billion parameter models and 500 strings for the 40 billion parameter model from the Wikitext dataset (Merity et al., 2016). The string lengths are uniformly distributed across lengths $[8, 10, 16, 22, 32]$ tokens.

Incremental Prompt Lengthening: To get a sense of the distribution of $k - \epsilon$ controllability for a range of k values, we performed multiple experiment rounds increasing $k = 0$ to 10. At each round, we applied the relevant prompt optimization method (greedy back generation for $k \leq 3$, GCG for $k > 3$) to generate optimized prompts. For the subsequent round, we eliminated solved Wikitext instances from the previous rounds, thus saving compute and gaining an understanding of the relationship between k and ϵ across a range of k values.

6 RESULTS

The portion of solved instances at each value of $k \in [0, 1, 2, 3, 4, 6, 8, 10]$ for Falcon-7b, Llama-7b, and Falcon-40b are shown in Figure 1. Across models, we find that roughly 40% of the problem instances are correct with no prompt ($k = 0$) and over 97% are correct with prompts of length $k \leq 10$. Concretely, Falcon-7b is $k - \epsilon$ controllable with $\epsilon = 0.0284$ for $k = 10$. Llama-7b has $\epsilon = 0.0136$ for $k = 10$, and Falcon-40b has $\epsilon = 0.030$ for $k = 10$.

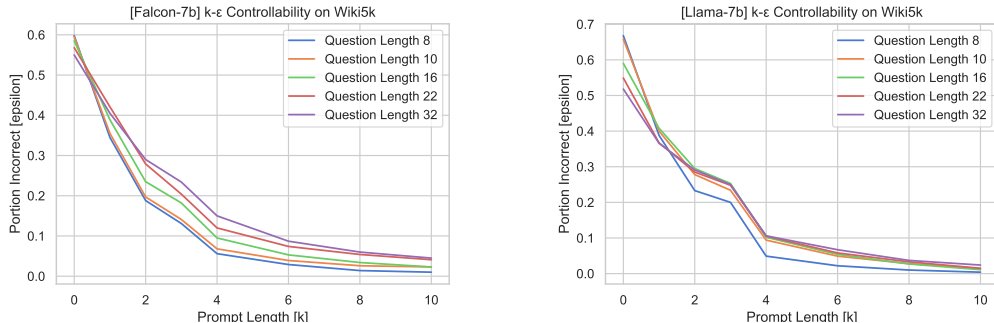
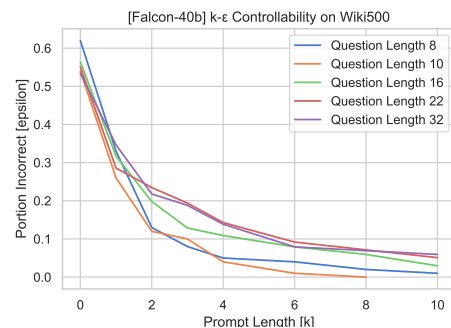


Figure 1: Main results on $k - \epsilon$ controllability.

Top left: $k - \epsilon$ values for Falcon-7b. 42.08% of the problem instances were correct with no prompt ($k = 0$) while 97.16% of the instances were solved with a prompt of length $k \leq 10$.

Top right: $k - \epsilon$ values for Llama-7b. 40.34% of the problem instances were correct with no prompt ($k = 0$) while 98.64% of the instances were solved with a prompt of length $k \leq 10$.

Bottom right: $k - \epsilon$ values for Falcon-40b. 43.8% of the problem instances were correct with no prompt ($k = 0$) while 97.0% were solved with a prompt of length $k \leq 10$.



The relationship between k and ϵ appears to be one of exponential decay: for each increment in the prompt length, some fraction of previously unsolved instances are solved. Within the bounds of the prompt lengths and question lengths studied, this fraction appears relatively stable. Plots of prompt length k versus $\log(\epsilon)$ can be found in Figure 2 in Appendix C where we observe a roughly linear relationship between k and $\log(\epsilon)$.

We observe a moderate positive correlation between the initial loss on the final token $\text{CE}(y, P_{LM}(y|x))$ and the number of prompt tokens k required to force the LLM to produce the correct answer (see Figure 3, 4, 5 in Appendix C) with an overall Pearson correlation score between 0.69-0.71 for each model. Importantly, there is substantial overlap in base loss across different k

values. Thus, while base loss on the final token is correlated with the number of tokens required to actualize control, it does not strictly determine the value of k .

Finally, we survey the most common tokens used in prompts for Falcon-7b, Llama-7b, and Falcon-40b in Figures 6, 7, and 8 in Appendix C. Interestingly, a long-tailed distribution appears, indicating that there is a small subset of the vocabulary that appears frequently across the optimal prompts. Many of the most common tokens are “special tokens” such as `<unk>`, `>>DOMAIN<<`, and `>>COMMENT<<`.

7 DISCUSSION

We proposed a control theoretic framework for understanding language model prompting, including the $k - \epsilon$ controllability measure. We proved a bound on the controllability of self-attention in terms of the singular values of its weight matrices, and we empirically measured the $k - \epsilon$ controllability of a panel of models on strings sampled from the Wikitext dataset where we found that the models are highly controllable, with over 97% of the instances solved with prompts of length $k \leq 10$. Moreover, our empirical results track with our expectations from the analytic results: ϵ (the portion of uncontrollable instances) decreases with the number of control tokens k in u and increases with the number of uncontrolled tokens in x .

Until now, it was unknown exactly how controllable LLMs are via prompting. Whereas previous works have optimized prompts for performance on zero-shot tasks (Shin et al., 2020; Zhou et al., 2023) or for LLM jailbreaks (Zou et al., 2023), we show the existence of short prompts (*magic words*) for the precise control of token generation across thousands of individual examples. We have demonstrated that language models are, in fact, highly controllable – immediately opening the door to the design of *LLM controllers* (programmatic or otherwise) that construct prompts on the fly to modulate LLM behavior. The behavior of LLMs is thus not strictly constrained by the weights of the model but rather by the sophistication of its prompt.

Our initial investigations provide an entry into the understanding of LLM controllability via prompts. However, a comprehensive understanding necessitates extending our exploration into diverse regimes. Exploring the controllability with longer prompts and longer questions (base token sequences) will be pivotal. Equally important is the study of diverse models to verify the generality of our findings. Our results indicate a similar level of controllability for the 40 billion parameter models as the 7 billion parameter models, with slightly less controllability for the large model. On the other hand, we only tested the large model on 500 sequences rather than 5000 due to computational constraints. Notably, the mean prompt length among solved Wikitext instances for Falcon-40b is 1.59 tokens, less than Falcon-7b (1.76 tokens) and Llama-7b (1.83 tokens). Moreover, the direct comparison of controllability scores of different model families is challenging since family uses a different tokenizer. The Llama family tokenizer, for instance, has a vocabulary of 30,000 tokens whereas the Falcon family has a vocabulary of 65,536 tokens. Further work is required to robustly compare controllability across models.

A particularly intriguing observation from our study is the log-linear relationship between prompt length k and controllability fraction ϵ (see Figure 2 in Appendix C). While this is compelling within our studied domain, it raises the essential question: is this relationship robust outside our current explorative scope? Unearthing universal scaling laws in LLM controllability would not only inform practical control applications but also open the door for theoretical insight into the nature of LLM behavior.

The progress we have made, both in understanding the bounds on self-attention controllability and the empirical measures of $k - \epsilon$ LLM controllability, underscores the potential of this control theoretic framing for studying LLMs. Below is a non-exhaustive list of open problems in LLM control, all stemming from the framing in section 3:

- **Control Properties of Chain-of-Thought:** Chain-of-Thought is a powerful technique where LLMs are allowed to generate intermediate tokens (i.e., “thoughts”) between a question and an answer (Wei et al., 2023). Along with its variants such as Tree of Thought (Yao et al., 2023) and Graph of Thought (Besta et al., 2023), it has been shown to significantly improve LLM performance on a range of tasks. The control properties of systems leverag-

ing these techniques is of great interest for understanding and composing systems of LLMs in the real world.

- **Stability of Chain-of-Thought:** Stability analysis is a foundational aspect of control theory (Sontag, 2013). Under what conditions does a system’s state $x \in \mathcal{X}$ or readout $y \in \mathcal{Y}$ stabilize to some asymptotic value or neighborhood? How can we design controllers that ensure stability? For LLM systems – particularly those employing chain-of-thought or other agentic paradigms – ensuring stability and minimizing hallucination is of great interest.
- **Distributional Control:** For a single-output LLM system, can we control the output distribution $P(y|x + u)$ to a desired distribution P^* over the vocabulary \mathcal{V} ? Can we force $D_{KL}(P(y|u + x) \| P^*) \leq \epsilon$ for some imposed ϵ cutoff? While we have demonstrated the ability to control the argmax of $P(y|u + x)$ through control input u , it remains unclear how much we are able to modulate this distribution beyond that.
- **Computational Cost of Control:** What are the performance characteristics of LLM control regularized by computational cost?
- **Learnability of Control:** To what extent can LLMs learn to control each other? Work such as Zhou et al. (2023) showed that LLMs are capable of human-level prompt engineering, but it is unclear how well an LLM can learn to control another when allowed to perform weight updates. Proximal policy optimization and other fine-tuning approaches are of great interest for this task, as this would allow controller models to learn about the nature of prompt-based control, unlike Zhou et al. (2023) that only applies pre-trained models to generate alternative prompts. Our preliminary experiments on PPO for training control models indicated that LLMs are capable of improving at controlling other models beyond their pre-trained capacity, but the maximal extent of this improvement remains unclear.
- **Controllable Subspaces:** In the control of linear dynamical systems, it is known that uncontrollable systems are often coordinate transformable into a representation where a subset of the coordinates are controllable and a subset are uncontrollable Sontag (2013). The existence (and interpretability) of these subspaces is of great interest for the full state controllability of LLMs as the structure of the controllable aspects may shed light on the nature of the intelligence exhibited by LLMs. Already we have shown that a controllable and uncontrollable components naturally emerge for self-attention heads in section 4 – can this be generalized to transformer blocks with nonlinearities and residual streams?
- **Composable LLM Systems:** One of the greatest boons of control theory is the ability to compose control modules and subsystems into an interpretable, predictable, and effective whole (Lian et al., 2002). The composition of LLM systems (potentially with non-LLM control modules) is an exciting avenue for scaling intelligent systems to maximally leverage the capabilities of LLMs. Depending on the aforementioned *learnability of control*, collectives of LLMs may well learn to function in the same hyper-controllable regime demonstrated herein, enabling horizontal scaling of performance.

8 CONCLUSION

We formalized prompt engineering as an optimal control problem on LLMs and introduced a general framework for LLM systems and controllability. In this framework, we define the $k - \epsilon$ controllability metric for measuring the steerability of LLMs with respect to an imposed text distribution. After proving a bound on the controllability of self-attention in terms of the singular values of its weight matrices, we computed the $k - \epsilon$ controllability of a panel of models.

Surprisingly, we found that optimal control prompts (*magic words*) of 10 tokens or less exist for over 97% of the WikiText causal language modelling (CLM) instances surveyed. Each magic word, when prepended to the CLM instance, forces the model to predict the correct final token in the sequence. Despite prior efforts on prompt optimization for improving LLM performance on zero-shot objectives, it was unknown until now exactly how controllable LLMs are via prompting. Our results indicate that the behavior of LLMs is not solely constrained by the weights of the model, but also by the sophistication of the prompt. We find the control theoretic framework for analyzing LLMs fruitful both for addressing practical issues with prompting and for generating fundamental insights and useful lines of inquiry as to the nature of these models.

REFERENCES

- Ebtesam Almazrouei, Hamza Alobeidli, Abdulaziz Alshamsi, Alessandro Cappelli, Ruxandra Cojocaru, Merouane Debbah, Etienne Goffinet, Daniel Heslow, Julien Launay, Quentin Malartic, Badreddine Noune, Baptiste Pannier, and Guilherme Penedo. Falcon-40B: an open large language model with state-of-the-art performance. 2023.
- Sebastian Anița, Viorel Arnăutu, Vincenzo Capasso, and Vincenzo Capasso. *An introduction to optimal control problems in life sciences and economics: From mathematical models to numerical simulation with MATLAB®*, volume 2. Springer, 2011.
- Yuntao Bai, Andy Jones, Kamal Ndousse, Amanda Askell, Anna Chen, Nova DasSarma, Dawn Drain, Stanislav Fort, Deep Ganguli, Tom Henighan, et al. Training a helpful and harmless assistant with reinforcement learning from human feedback. *arXiv preprint arXiv:2204.05862*, 2022.
- Maciej Besta, Nils Blach, Ales Kubicek, Robert Gerstenberger, Lukas Gianinazzi, Joanna Gajda, Tomasz Lehmann, Michal Podstawska, Hubert Niewiadomski, Piotr Nyczyk, and Torsten Hoefer. Graph of thoughts: Solving elaborate problems with large language models, 2023.
- Tom Brown, Benjamin Mann, Nick Ryder, Melanie Subbiah, Jared D Kaplan, Prafulla Dhariwal, Arvind Neelakantan, Pranav Shyam, Girish Sastry, Amanda Askell, Sandhini Agarwal, Ariel Herbert-Voss, Gretchen Krueger, Tom Henighan, Rewon Child, Aditya Ramesh, Daniel Ziegler, Jeffrey Wu, Clemens Winter, Chris Hesse, Mark Chen, Eric Sigler, Mateusz Litwin, Scott Gray, Benjamin Chess, Jack Clark, Christopher Berner, Sam McCandlish, Alec Radford, Ilya Sutskever, and Dario Amodei. Language models are few-shot learners. In H. Larochelle, M. Ranzato, R. Hadsell, M.F. Balcan, and H. Lin (eds.), *Advances in Neural Information Processing Systems*, volume 33, pp. 1877–1901. Curran Associates, Inc., 2020. URL https://proceedings.neurips.cc/paper_files/paper/2020/file/1457c0d6bfcb4967418bfb8ac142f64a-Paper.pdf.
- Tianle Cai, Xuezhi Wang, Tengyu Ma, Xinyun Chen, and Denny Zhou. Large language models as tool makers, 2023.
- Ian J. Goodfellow, Jonathon Shlens, and Christian Szegedy. Explaining and harnessing adversarial examples, 2015.
- Chuan Guo, Alexandre Sablayrolles, Hervé Jégou, and Douwe Kiela. Gradient-based adversarial attacks against text transformers, 2021.
- Thilo Hagendorff. Machine psychology: Investigating emergent capabilities and behavior in large language models using psychological methods, 2023.
- Zhengbao Jiang, Frank F. Xu, Jun Araki, and Graham Neubig. How can we know what language models know?, 2020.
- Feng-Li Lian, James Moyne, and Dawn Tilbury. Network design consideration for distributed control systems. *IEEE transactions on control systems technology*, 10(2):297–307, 2002.
- Stephen Merity, Caiming Xiong, James Bradbury, and Richard Socher. Pointer sentinel mixture models, 2016.
- David Noever and Forrest McKee. Numeracy from literacy: Data science as an emergent skill from large language models, 2023.
- OpenAI, Nov 2022. URL <https://openai.com/blog/chatgpt>.
- OpenAI. Gpt-4 technical report, 2023.
- Fabio Petroni, Tim Rocktäschel, Patrick S. H. Lewis, Anton Bakhtin, Yuxiang Wu, Alexander H. Miller, and Sebastian Riedel. Language models as knowledge bases? *CoRR*, abs/1909.01066, 2019. URL <http://arxiv.org/abs/1909.01066>.

Laria Reynolds and Kyle McDonell. Prompt programming for large language models: Beyond the few-shot paradigm, 2021.

Sandip Roy, Yan Wan, and Ali Saberi. A network control theory approach to virus spread mitigation. In *2009 IEEE Conference on Technologies for Homeland Security*, pp. 599–606, 2009. doi: 10.1109/THS.2009.5168092.

Baptiste Rozière, Jonas Gehring, Fabian Gloeckle, Sten Sootla, Itai Gat, Xiaoqing Ellen Tan, Yossi Adi, Jingyu Liu, Tal Remez, Jérémie Rapin, Artyom Kozhevnikov, Ivan Evtimov, Joanna Bitton, Manish Bhatt, Cristian Canton Ferrer, Aaron Grattafiori, Wenhan Xiong, Alexandre Défossez, Jade Copet, Faisal Azhar, Hugo Touvron, Louis Martin, Nicolas Usunier, Thomas Scialom, and Gabriel Synnaeve. Code llama: Open foundation models for code, 2023.

Weijia Shi, Xiaochuang Han, Hila Gonen, Ari Holtzman, Yulia Tsvetkov, and Luke Zettlemoyer. Toward human readable prompt tuning: Kubrick’s the shining is a good movie, and a good prompt too?, 2022.

Taylor Shin, Yasaman Razeghi, Robert L. Logan IV au2, Eric Wallace, and Sameer Singh. Auto-prompt: Eliciting knowledge from language models with automatically generated prompts, 2020.

Eduardo D Sontag. *Mathematical control theory: deterministic finite dimensional systems*, volume 6. Springer Science & Business Media, 2013.

Wilson L. Taylor. “cloze procedure”: A new tool for measuring readability. *Journalism Quarterly*, 30(4):415–433, 1953. doi: 10.1177/107769905303000401. URL <https://doi.org/10.1177/107769905303000401>.

Hugo Touvron, Thibaut Lavril, Gautier Izacard, Xavier Martinet, Marie-Anne Lachaux, Timothée Lacroix, Baptiste Rozière, Naman Goyal, Eric Hambro, Faisal Azhar, Aurelien Rodriguez, Armand Joulin, Edouard Grave, and Guillaume Lample. Llama: Open and efficient foundation language models, 2023.

Ashish Vaswani, Noam Shazeer, Niki Parmar, Jakob Uszkoreit, Llion Jones, Aidan N Gomez, Łukasz Kaiser, and Illia Polosukhin. Attention is all you need. *Advances in neural information processing systems*, 30, 2017.

Longyue Wang, Chenyang Lyu, Tianbo Ji, Zhirui Zhang, Dian Yu, Shuming Shi, and Zhaopeng Tu. Document-level machine translation with large language models. *arXiv preprint arXiv:2304.02210*, 2023a.

Zengzhi Wang, Qiming Xie, Zixiang Ding, Yi Feng, and Rui Xia. Is chatgpt a good sentiment analyzer? a preliminary study. *arXiv preprint arXiv:2304.04339*, 2023b.

Jason Wei, Yi Tay, Rishi Bommasani, Colin Raffel, Barret Zoph, Sebastian Borgeaud, Dani Yogatama, Maarten Bosma, Denny Zhou, Donald Metzler, Ed H. Chi, Tatsunori Hashimoto, Oriol Vinyals, Percy Liang, Jeff Dean, and William Fedus. Emergent abilities of large language models, 2022.

Jason Wei, Xuezhi Wang, Dale Schuurmans, Maarten Bosma, Brian Ichter, Fei Xia, Ed Chi, Quoc Le, and Denny Zhou. Chain-of-thought prompting elicits reasoning in large language models, 2023.

Yuxin Wen, Neel Jain, John Kirchenbauer, Micah Goldblum, Jonas Geiping, and Tom Goldstein. Hard prompts made easy: Gradient-based discrete optimization for prompt tuning and discovery, 2023.

Jason Weston, Antoine Bordes, Sumit Chopra, and Tomás Mikolov. Towards ai-complete question answering: A set of prerequisite toy tasks. In Yoshua Bengio and Yann LeCun (eds.), *4th International Conference on Learning Representations, ICLR 2016, San Juan, Puerto Rico, May 2-4, 2016, Conference Track Proceedings*, 2016. URL <http://arxiv.org/abs/1502.05698>.

Shunyu Yao, Dian Yu, Jeffrey Zhao, Izhak Shafran, Thomas L. Griffiths, Yuan Cao, and Karthik Narasimhan. Tree of thoughts: Deliberate problem solving with large language models, 2023.

Tau-Mu Yi, Yun Huang, Melvin I Simon, and John Doyle. Robust perfect adaptation in bacterial chemotaxis through integral feedback control. *Proceedings of the National Academy of Sciences*, 97(9):4649–4653, 2000.

Hanqing Zhang, Haolin Song, Shaoyu Li, Ming Zhou, and Dawei Song. A survey of controllable text generation using transformer-based pre-trained language models. *CoRR*, abs/2201.05337, 2022. URL <https://arxiv.org/abs/2201.05337>.

Yongchao Zhou, Andrei Ioan Muresanu, Ziwen Han, Keiran Paster, Silviu Pitis, Harris Chan, and Jimmy Ba. Large language models are human-level prompt engineers, 2023.

Andy Zou, Zifan Wang, J. Zico Kolter, and Matt Fredrikson. Universal and transferable adversarial attacks on aligned language models, 2023.

A PROOF OF SELF-ATTENTION CONTROLLABILITY BOUND

Attention Matrix Decomposition: We begin by observing the block structure of the attention matrix. Let us break down the computation of the attention matrix into the unnormalized attention matrix $\mathbf{A} = \mathbf{Q}\mathbf{K}^\top$ and the subsequent row-wise softmax normalized attention matrix $\tilde{\mathbf{A}}$.

$$\tilde{\mathbf{A}} = [\alpha_{ij}] \quad \text{where} \quad \alpha_{ij} = \frac{\exp\left(\frac{q_i \cdot k_j}{\sqrt{d_k}}\right)}{\sum_{\ell=1}^{N+M} \exp\left(\frac{q_i \cdot k_\ell}{\sqrt{d_k}}\right)} \quad (6)$$

We can partition $\tilde{\mathbf{A}}$ into four quadrants based on whether the queries and keys in the numerator of α_{ij} are derived from $\mathbf{u}_{1:N}$ or $\mathbf{x}_{1:M}$:

$$\tilde{\mathbf{A}} = \begin{bmatrix} \tilde{\mathbf{A}}_{uu} & \tilde{\mathbf{A}}_{ux} \\ \tilde{\mathbf{A}}_{xu} & \tilde{\mathbf{A}}_{xx} \end{bmatrix} \quad (7)$$

Expressing $\mathbf{x}'_{1:M}$ in terms of the block matrices, we get

$$\mathbf{x}^* = \mathbf{x}' = \underbrace{\tilde{\mathbf{A}}_{xu}(\mathbf{u}\mathbf{W}_v)}_{\mathbf{x}^{(1)} \in \mathbb{R}^{M \times d_{out}}} + \underbrace{\tilde{\mathbf{A}}_{xx}(\mathbf{x}\mathbf{W}_v)}_{\mathbf{x}^{(2)} \in \mathbb{R}^{M \times d_{out}}} \quad (8)$$

Disentangling $\mathbf{x}^{(1)}, \mathbf{x}^{(2)}$: These two components $\mathbf{x}^{(1)}, \mathbf{x}^{(2)}$ are not entirely independent, however. The denominator of the softmax is still affected by all members of the row, so both are affected by the control input \mathbf{u} and the imposed input \mathbf{x} . Importantly, the control input \mathbf{u} only shows up in the denominator of $\tilde{\mathbf{A}}_{xx}$ and nowhere else in $\mathbf{x}^{(2)}$. We can separate $\mathbf{x}^{(1)}, \mathbf{x}^{(2)}$ into a controllable component $\hat{\mathbf{x}}^{(1)}$ and uncontrollable component $\hat{\mathbf{x}}^{(2)}$ by decomposing the denominator in Equation 6 for each row i in as

$$D_i = \underbrace{\sum_{\ell=1}^N \exp\left(\frac{q_i \cdot k_\ell}{\sqrt{d_k}}\right)}_{D_i^{(1)}} + \underbrace{\sum_{\ell=N+1}^{N+M} \exp\left(\frac{q_i \cdot k_\ell}{\sqrt{d_k}}\right)}_{D_i^{(2)}} \quad (9)$$

Let $\mathbf{D} = \text{diag}\{D_i\}_{i=N+1}^{N+M}$, $\mathbf{D}^{(1)} = \text{diag}\{D_i^{(1)}\}_{i=N+1}^N$, and $\mathbf{D}^{(2)} = \text{diag}\{D_i^{(2)}\}_{i=N+1}^{N+M}$. All of these are square $M \times M$ matrices with non-negative entries.

We can now “unnormalize” $\mathbf{x}^{(1)}, \mathbf{x}^{(2)}$ such that $\hat{\mathbf{x}}^{(2)}$ is independent of the control input $\mathbf{u}_{1:N}$:

$$\hat{\mathbf{x}}^{(1)} = \mathbf{D}\mathbf{D}^{(1)-1} \underbrace{\tilde{\mathbf{A}}_{xu}\mathbf{u}\mathbf{W}_v}_{\mathbf{x}^{(1)}} \quad (10)$$

$$\hat{\mathbf{x}}^{(2)} = \mathbf{D}\mathbf{D}^{(2)-1} \underbrace{\tilde{\mathbf{A}}_{xu}\mathbf{x}\mathbf{W}_v}_{\mathbf{x}^{(2)}} \quad (11)$$

Now $\hat{\mathbf{x}}^{(2)}$ is equivalent to the output of the transformer if only \mathbf{x} were used as inputs (no influence from control signal \mathbf{u}). $\hat{\mathbf{x}}^{(1)}$ is also now the only term that depends on control input \mathbf{u} .

We can now express the condition in equation 8 in a disentangled manner and isolate the controllable $\hat{\mathbf{x}}^{(1)}$:

$$\mathbf{x}^* = \mathbf{D}^{(1)}\mathbf{D}^{-1}\hat{\mathbf{x}}^{(1)} + \mathbf{D}^{(2)}\mathbf{D}^{-1}\hat{\mathbf{x}}^{(2)} \quad (12)$$

$$\implies \hat{\mathbf{x}}^{(1)} = \mathbf{x}^* + \underbrace{\mathbf{D}^{(2)}\mathbf{D}^{(1)-1}(\mathbf{x}^* - \hat{\mathbf{x}}^{(2)})}_{\text{Explosive!}} \quad (13)$$

Notably, the right most term is liable to explode for $D_i^{(1)} \ll D_i^{(2)}$.

We now know the value of \mathbf{x}^* (imposed), $\mathbf{D}^{(2)}, \hat{\mathbf{x}}^{(2)}$ (functions only of imposed \mathbf{x}). Assuming some bounds on the input vectors (e.g., $\|u_i\| \leq 1$ and $\|x_i\| \leq 1$), we can bound the remaining terms $\hat{\mathbf{x}}^{(1)}$ and $\mathbf{D}^{(1)}$.

Bounds on $D_i^{(1)}$: Due to the constraints $\|x_i\| \leq 1$ and $\|y_i\| \leq 1$, the maximum value for $D_i^{(1)}$ as defined in equation 9 occurs when the query and keys in question align with the maximal singular value of the W_q, W_k matrices respectively.

$$\exp\left(\frac{q_i \cdot k_\ell}{\sqrt{d_k}}\right) \leq \exp\left(\frac{\sigma_{\max}(W_q)\sigma_{\max}(W_k)}{\sqrt{d_k}}\right) \quad (14)$$

$$\implies D_i^{(1)} \leq N \exp\left(\frac{\sigma_{\max}(W_q)\sigma_{\max}(W_k)}{\sqrt{d_k}}\right) \quad (15)$$

Bounds on $\hat{\mathbf{x}}_i^{(1)}$: Each $\hat{\mathbf{x}}_i^{(1)}$ must lie in the convex hull of the value vectors $v_1 \dots v_N$ associated with $u_1 \dots u_N$. Since each $\|u_i\| \leq 1$, the maximal value vector would be

$$\max_{i \in [N]} \|W_v u_i\| = \max_{i \in [N]} \|v_i\| \leq \sigma_{\max}(W_v) \quad (16)$$

This implies that $\|\hat{\mathbf{y}}_i^{(1)}\| \leq \sigma_{\max}(W_v)$.

Resulting Bound on Controllability: $D_i^{(2)}$ is a function only of the uncontrolled $\mathbf{x} = x_1 \dots x_M$ inputs. We have shown bounds on each $\|\hat{\mathbf{x}}_i^{(1)}\|$ and $D_i^{(1)}$. We can conclude that the system will be **strictly uncontrollable** if

$$\sigma_{\max}(W_v) < \left\| \mathbf{x}_i^* + \left(\frac{D_i^{(2)}}{N \exp\left(\frac{\sigma_{\max}(W_q)\sigma_{\max}(W_k)}{\sqrt{d_k}}\right)} \right) (\mathbf{x}_i^* - \hat{\mathbf{x}}_i^{(2)}) \right\| \quad (17)$$

This condition is liable to arise when $M \gg N$. Intuitively, this condition is met when the attention mechanism allocates a substantial amount of attention to the values arising from the uncontrolled $x_1 \dots x_M$ inputs (i.e., large $D_i^{(2)}$) with very few controllable inputs $u_1 \dots u_N$ to the point that even maximal attention allocation to the $u_1 \dots u_N$ values could not steer the system to the goal state.

B PROMPT OPTIMIZATION ALGORITHMS

Algorithm 1 Greedy Token-Wise Prompt Generation

Require: A causal LLM P_{LM} with vocabulary \mathcal{V} , a set of base tokens $x \in \mathcal{V}^n$, a desired final token $y \in \mathcal{V}$, and a desired number of prompt tokens k .

Ensure: Magic words u^* of length k .

- 1: Initialize u^* to be empty.
- 2: **for** i from 1 to k **do**
- 3: **for all** $u' \in \mathcal{V}$ **do**
- 4: compute $P_{LM}(y|u' + u^* + x)$
- 5: **end for**
- 6: Select the u' that maximizes the probability of y given $u' + u^* + x$. Prepend u' to u^*
- 7: **end for**
- 8: **return** u^*

Algorithm 2 Greedy Coordinate Gradient

Require: A causal LLM P_{LM} that accepts token strings from a vocabulary \mathcal{X} , an embedding dictionary \mathbf{e} , embeddings \mathbf{e}_i^* corresponding to each token i of u^* , a set of base tokens $x_{1:n}$, a desired number of prompt tokens k , iterations T , k_{sub} , and batch size B .

Ensure: Magic words u^* of length k .

- 1: Initialize u^* to be random tokens from vocabulary.
- 2: **for** iteration from 1 to T **do**
- 3: **for** i from 1 to k **do** ▷ Compute the top k_{sub} most promising substitutions.
- 4: $\mathcal{X}_i = \text{Top-}k_{sub}(\mathbf{e}^T \nabla_{\mathbf{e}_i^*} P_{LM}(x_n|u^* + x_{1:n-1}))$
- 5: **end for**
- 6: **for** b from 1 to B **do**
- 7: $i = \text{randint}([1, \dots, k])$ ▷ Select random position to swap.
- 8: $j = \text{randint}([1, \dots, k_{sub}])$ ▷ Select random token from candidate set.
- 9: $\tilde{u}_b^*[i] = \mathcal{X}_i[j]$ ▷ Swap token at position i .
- 10: **end for**
- 11: $u^* = \tilde{u}_b^*$, where $b^* = \text{argmax}_b(P_{LM}(x_n|u^* + x_{1:n-1}))$ ▷ Select replacement which maximizes probability of future token.
- 12: **end for**
- 13: **return** u^*

C SUPPLEMENTARY FIGURES: OPTIMAL CONTROL PROMPTS

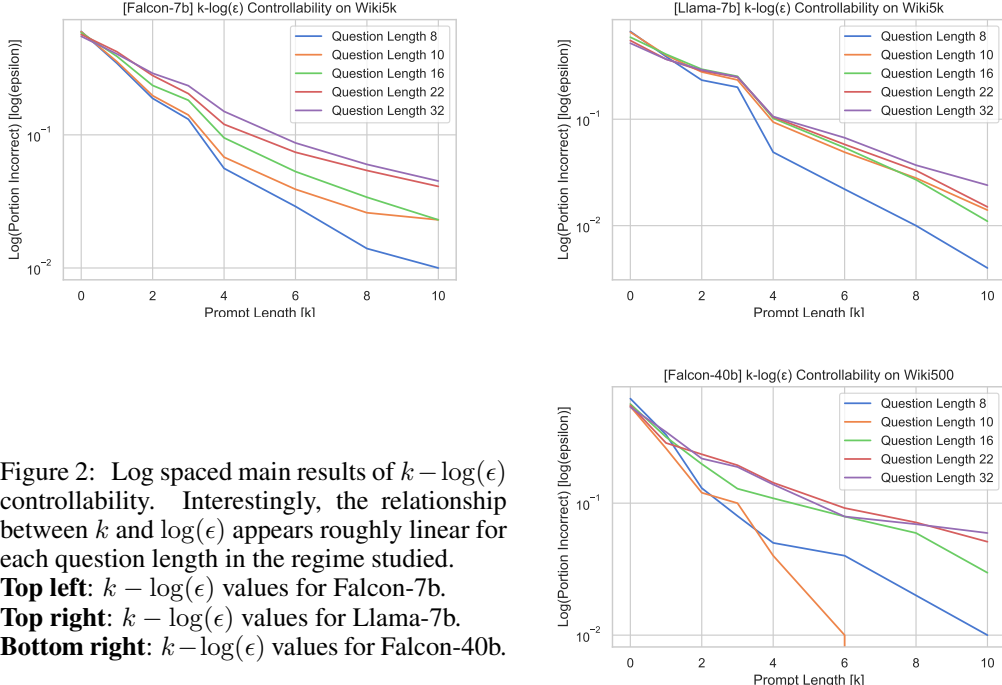


Figure 2: Log spaced main results of $k - \log(\epsilon)$ controllability. Interestingly, the relationship between k and $\log(\epsilon)$ appears roughly linear for each question length in the regime studied.

Top left: $k - \log(\epsilon)$ values for Falcon-7b.

Top right: $k - \log(\epsilon)$ values for Llama-7b.

Bottom right: $k - \log(\epsilon)$ values for Falcon-40b.

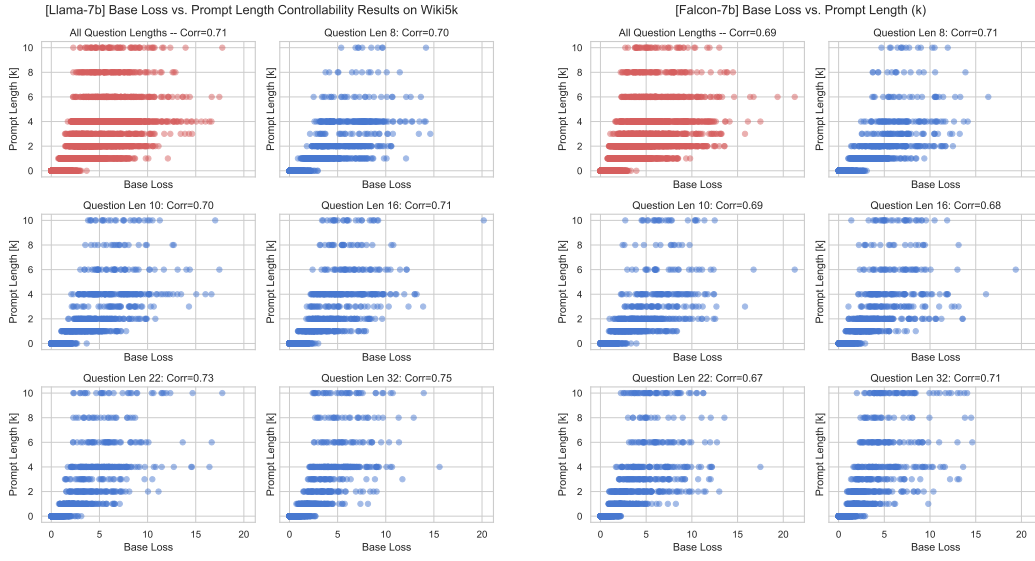


Figure 3: Prompt length k versus base cross-entropy loss on the final token for Llama-7b.

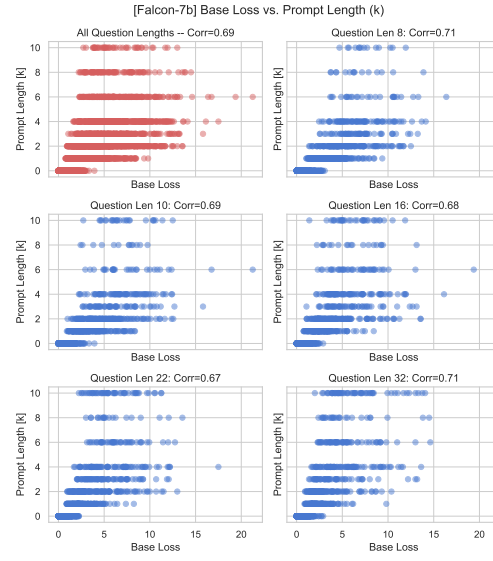


Figure 4: Prompt length k versus base cross-entropy loss on the final token for Falcon-7b.

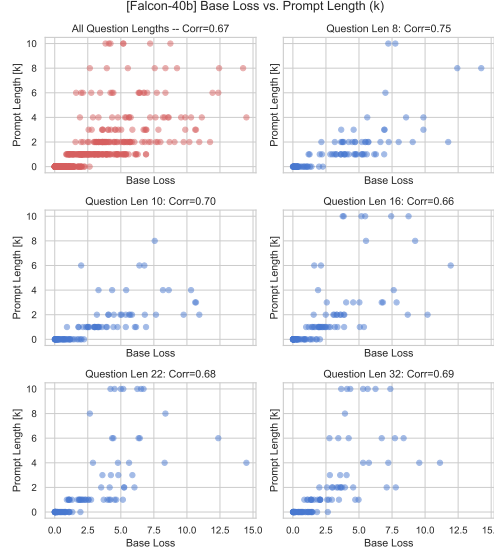


Figure 5: Prompt length k versus base cross-entropy loss on the final token for Falcon-40b.

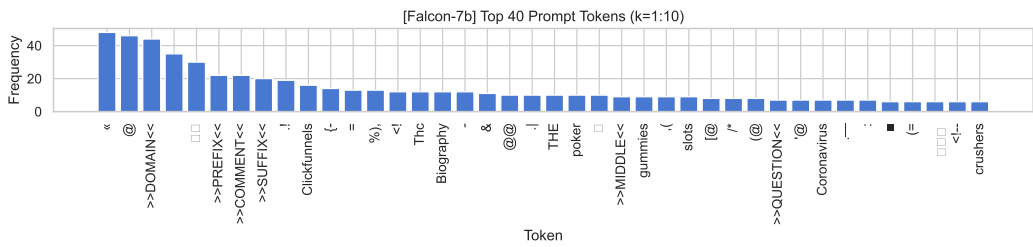


Figure 6: Prompt token frequencies for Falcon-7b across Wikitext5k instances for $k = 1 : 10$.

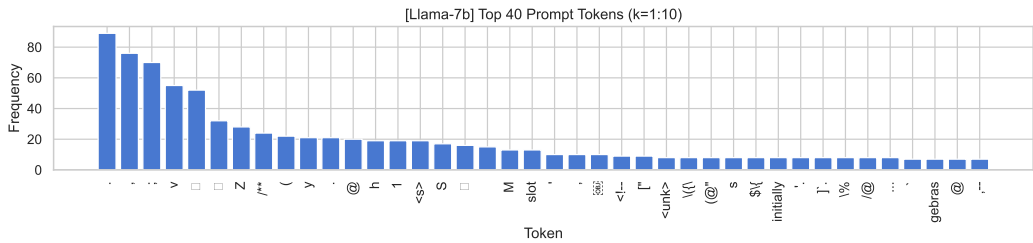


Figure 7: Prompt token frequencies for Llama-7b across Wikitext5k instances for $k = 1 : 10$.

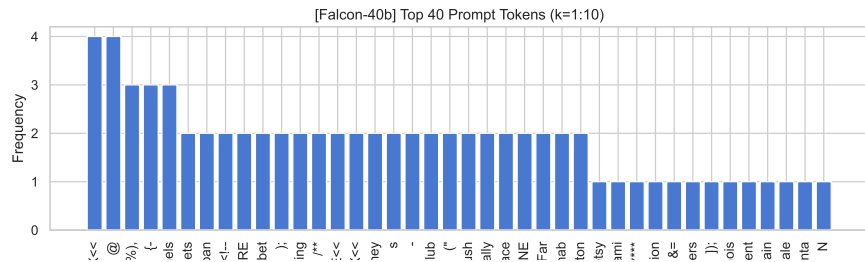


Figure 8: Prompt token frequencies for Falcon-40b across Wikitext500 instances for $k = 1 : 10$.